行政院國家科學委員會補助專題研究計畫□ 成 果 報 告 ■期中進度報告

利用基因體與蛋白質體學方法探討抗腸病毒71型之機轉: 中藥陳皮與衍生的類黃酮天然藥物的影響（第2年）

計畫類別：■ 個別型計畫　□ 整合型計畫
計畫編號：NSC 97 － 2320 － B － 039 － 023 －MY3
執行期間： 98 年 08 月 01 日至 99 年 07 月 31 日

計畫主持人：林應如

共同主持人：林昭庚、蔡輔仁、萬磊、賴建成、林振文、許晉銓、侯鈺琪。

計畫參與人員：林亭旭、雷玉潔、林欣誼。

成果報告類型(依經費核定清單規定繳交)：■精簡報告　□完整報告

本成果報告包括以下應繳交之附件：
□赴國外出差或研習心得報告一份
□赴大陸地區出差或研習心得報告一份
□出席國際學術會議心得報告及發表之論文各一份
□國際合作研究計畫國外研究報告書一份
處理方式：除產學合作研究計畫、提升產業技術及人才培育研究計畫、列管計畫及下列情形者外，得立即公開查詢
■涉及專利或其他智慧財產權，□一年■二年後可公開查詢

執行單位：中國醫藥大學 中國醫學研究所

中 華 民 國 99 年 05 月 31 日

中文摘要:

腸病毒71型是微小病毒科家族中最重要的病原之一。它能造成嚴重的併發症如腦炎，肺水腫甚至死亡。至今臨床上還沒有有效藥物用來抑制或治療腸病毒71型感染。我們的初步研究結果顯示(1) 中藥陳皮與衍生的類黃酮天然藥物具有抗腸病毒71型活性 (2) 利用基因微陣列與蛋白質體方法鑑定出一些參與腸病毒71型與RD細胞株交互作用的細胞標的物。有鑑於此，我們假設一些經由中藥陳皮與衍生的類黃酮天然藥物誘導之細胞標的物對於參與病毒與細胞交互作用與抗病毒機轉能產生影響。為了證實此假說，我們希望藉由功能性基因體學- 基因微陣列、二維電泳、奈米毛細管質譜儀、即時核酸偵測儀、免疫轉置、基因抑制與基因復原等技術來闡明這些藥物的抗腸病毒71型之分子機轉影響。我們已利用microarray and proteomic 方法找出與EV71感染相關蛋白。利用相同方法，接下來要找出與Kaempferol藥物相關的細胞蛋白。利用siRNA與cDNA reconstruction assays，我們要証明這些candidate細胞蛋白在抗EV71之中藥相關研究上有幫助。此研究能進一步了解抗病毒71 型感染的分子作用機制。此假說若能被驗證則能對於抗病毒71型感染藥物的發展與公共衛生問題的解決有幫助。

英文摘要:

Enterovirus 71 (EV71) is one of the most important pathogens in the family of *Picornaviridae* that can cause severe complications, such as encephalitis, pulmonary edema and even death. To date, no effective drugs have been approved for clinical use. Our preliminary results has suggested that (1) *Pericarpium Citri Reticulatae* and herb-derived flavonoids herb extract possessed anti-EV71 activity, and (2) a novel sets of identified targets have been identified in EV71-RD cell interactions using microarray and proteomic analyses. We hypothesize that the cellular transcripts and proteins induced by *Pericarpium Citri Reticulatae* and herb-derived flavonoids may contribute to the complex network of virus-host interactions and cellular anti-viral processes. To test this hypothesis, we will use functional genomics- microarray, 2-DE and nanoscale capillary LC/ESI quadrupole-TOF MS, real-time RT-PCR, immunoblot and gene knockdown and gene reconstitution technologies to elucidate the molecular effects of these herb and herb-derived flavonoids in anti-EV71 therapies. To identify cellular proteins induced by EV71, which these cellular proteins may be involved in EV71 pathogenesis and possible anti-EV71 mechanism, both microarray and proteomic studies were used to identify cellular proteins induced by EV71 infection. The results are shown in Table 2 and Table 3. Our next step is to identify cellular proteins induced by Kaempferol using both microarray and proteomic studies. Combined with the results in Table 2 and Table 3, we hope to investigate the functions of these cellular proteins on anti-EV71 activity using siRNA and cDNA reconstruction assays.This study of characterizing the effect of the flavonoids will allow us to identify the molecular mechanisms involved in anti-EV71 infection. This information could be useful for developing anti-viral drugs against EV71 infection and contributing to the public health problem.

報告內容:

前言與文獻探討:

Enterovirus 71 (EV71) is one of the most important pathogens in the family of *Picornaviridae* that can cause severe complications in the post-poliovirus era, such as encephalitis, pulmonary edema and even death. EV71 is an endemic enterovirus with a global distribution--- in Asia (3, 19, 21, 28, 35), Australia (16, 23), Europe (5, 31) and the United States (1, 4, 17). In 1998, an EV71 epidemic occurred in Taiwan, affecting 120,000 children in Taiwan (3, 19, 20, 27). Of the 320 children who were hospitalized with acute neurological disease and 78 children were killed. Children under 5 years old are particularly susceptible to the most severe EV71-associated neurological complications. Once the central nervous system is infected, a patient can die very quickly from encephalitis and pulmonary edema.

Since the children's health is threatened by EV71 infection, the development of strategies to prevent or treat EV71 infection should be very essential. Although it is generally known that viral, hot and environmental factors contribute to the pathogenesis and progression of EV71 infection, the interplay between the virus and host cells remains poorly understand. Investigations to a better understanding of cellular events that follow EV71 infection are likely to provide insights that will facilitate the development of such strategies. The interactions between the virus and host cells are complex and multifaceted. The virus has developed mechanisms to counteract the host cell response and utilized host cell machinery to support efficient viral replication. In contrast, the host cellular response to viral infection represents a complex of divergent pathways designed to eliminate the virus and protect the host. The pathways in response to virus infection may modulate the expression of cell surface molecules and perturb the host transcription and translation machinery. However, these vigorous changes can result in either dysfunction or death of infected cells and may contribute to the pathogenesis of EV71 infection. The viral and cellular factors that determine the outcome are still unknown.

No anti-viral drugs have been approved by FDA for the treatment of EV71 infection. Clinical treatments are directed toward symptomatic relief of the most prominent symptoms of each clinical syndrome. Developing effective anti-viral drugs against EV71 infection seems to contribute to this public health problem. Herbal therapy has been an important issue in traditional Chinese medicine with anti-cancer, anti-viral, anti-bacterial and anti-inflammatory properties (12, 24, 26, 29). Herbal intervention is now widespread in all regions of the developing world and is rapidly growing in industrialized countries (2, 10, 11, 39). Furthermore, herbal plants are good sources of natural compounds and are of interest as possible sources to control viral infection. Several hundred herbal plants have been reported to have strong anti-viral activity and some of them have already been used to treat animals and people who suffer from viral infection (41, 42). Despite broad use, there are still insufficient molecular mechanisms about how they work to possess anti-viral activities. Lack of scientific evidence showing the molecular pathways of their action diminishes their clinical utility. Therefore, basic research aimed at elucidating the mechanisms of action underlying the herbal effects should have a high priority.

Pericarpium Citri Reticulatae is a herb that is widely used in traditional Chinese medicine as promoting the Liver Qi activity and the function of digestive system (9, 12, 29). *Pericarpium Citri Reticulatae* belongs to the *Citrus* species and contains active components of flavonoids. Recently, the flavonoids derived from this herb have been reported to have a broad anti-enterovirus spectrum of activity, efficiently inhibiting human rhinovirus, Sabin type 2 poliovirus, hepatitis A virus, coxsackievirus B4 and echovirus 6 infections (6, 7, 15, 34). Because *Pericarpium Citri Reticulatae* and herb-derived flavonoids have the anti-enterovirus property, we hypothesized that these agents may also have the similar inhibition effect on EV71 infection. In addition, the role of these herb and herb-derived drugs actions on the anti-viral activity has not been established.

Functional genomics, an part of the new drug-discovery process, have had a marked impact on human infectious disease research (8, 25). The technologies used in functional genomics include gene profiling, proteomics and gene knockdown assays.

Gene profiling (also called DNA microarray) is one of the highest-throughput methods for functionalizing the genome (36). RNA extracted from cells or tissues is converted into cDNA and labeled. The labeled cDNA is hybridized to the probes and the label bound to each probe is determined. In influenza virus-host cells interaction studies, the microarray assay revealed that the expression of numerous cellular genes, including genes involved in transcriptional regulation, growth-factor signaling, mRNA processing, protein synthesis and protein degradation have been altered by influenza virus infection (13). Furthermore, the microarray analyses have also been applied in a broad range of virus experimental systems, including HCV NS5A-expressing cell lines, the HCV replicon system and HCV-infected cirrhotic livers (14, 38). Recently, the addition of proteomic analyses provides a clearer picture in protein level to characterize protein interaction networks and cellular changes on a global scale.

Proteomics is used to determine differential protein expression, post-translational modifications and alternative splicing and processed products. Two-dimensional gel electrophoresis (2-DE) is used to fractionate the numerous proteins from a cell or tissue and to identify differentially expressed or modified proteins. Followed by mass spectrometry, the individual protein spots of interest from the gels are identified. In Dengue virus-host cells interaction studies, the proteomic analysis showed that most of the altered proteins were the key factors involved in transcription and translation processes (33). Furthermore, the proteomic analyses have also been applied in the effects of individual viral proteins on the cellular proteome. 2D gel analysis showed that 20 cellular proteins changes in cellular protein levels before and after the expression of a single EBV protein, EBNA2 (37). This approach provides valuable information on viral pathogenesis and life cycles as well as new insights into cellular functions.

Gene profiling and proteomic analyses provide us a global perspective on the virus-host interactions from gene expression to protein production. However, these analyses are not an end point but rather are a starting point for functional studies. Recent functional studies to investigate a particular gene are to inhibit its target mRNA by using anti-sense oligonucleotides. The anti-sense

oligonucleotides technology (also called gene knockdown methods) include anti-sense RNA and RNA interference (RNAi) (18, 30). The translation of the mRNA is inhibited by several mechanisms including degradation of the mRNA, interference with the splicing process or a physical blocking of the translational machinery. In viral systems, siRNA targeted against viral or host cell genes has been successfully used to inhibit viral replication. In HIV studies, siRNA duplexes targeted against HIV genes inhibit HIV replication (22, 32). Moreover, targeting of the downstream nuclear factor κB (NF-κB) p65 gene decreased HIV replication (40). In conclusion, the functional characterization in gene inhibition by anti-sense and siRNA significantly facilitate the validation of a large number of potential target genes identified by DNA microarrays or proteomic methods.

研究目的:

Our current working model, sketched below, illustrates that *Pericarpium Citri Reticulatae* and herb-derived flavonoids participate in anti-EV71 activity via unknown host target genes. Cells are mocked infected, infected with EV71 and treated with *Pericarpium Citri Reticulatae* and herb-derived flavonoids. The up-regulated and down-regulated host target genes, which in turn contribute to virus-host interactions or cellular anti-viral processes, are identified by the comparison of cells only control. Finding of host target genes would significantly improve our understanding of *Pericarpium Citri Reticulatae* and herb-derived flavonoids in anti-EV71 activity. Further confirmation of these target genes would facilitate the mechanisms of action underlying these drugs effects against EV71 infection and anti-EV71-related diagnostic and therapeutic development.

研究方法:

Cell lines and virus

The cells are incubated at 37℃ in minimal essential medium supplemented with 10% fetal bovine serum and 100 IU/ml of penicillin and 100 μg/ml of streptomycin. Our EV71 virus isolated

from the clinical specimen of young patient in China Medical University Hospital was identified and used in this study. The EV71 virus used in our experiments was propagated in RD cells and stored at -70℃. Viral titers are determined as median tissue culture infective dose ($TCID_{50}$) per ml in confluent RD cells in 96-well microtiter plates.

Construction of the bicistronic mRNA assay system

The pCDNA3.1 plasmid for bicistronic mRNA system construction contains CMV promoter. The LUC gene is cloned behind the CMV promoter. The viral IRES variant genes are cloned behind the LUC gene, respectivity. The SEAP gene is cloned behind the viral IRES genes. The plasmid contains all the gene constructs described above is then transfected into RD cells. After 24 h, the culture medium and cell lysate are collected for SEAP and LUC activity analysis.

Evaluation of the bicistronic mRNA assay system

The plasmid contains all the gene constructs descrived above is then transfected into RD cells. After 24 h, the varing concentrations of the drug are added to the culture medium for 24 h incubation. The culture medium and cell lysate are then collected for SEAP and LUC activity analysis.

Microarray analysis

Human genome-wide gene expression is examined with the GeneChip system HG-U133 microarray (Affymetrix Inc., Santa Clara, CA), which is composed of more than 22,000 oligonucleotide probe sets interrogating approximately 18,400 unique transcripts, including 14,500 well-characherized human genes. Quality control, GeneChip hybridization and data acquisition and analysis are performed according to the standard protocols available from Affymetrix. In brief, total RNAs of the cells only control, EV71-infected cells and herb and herb-derived treated cells are extracted using RNeasy minikit (Qiagen, Valencia, CA). Double-stranded cDNA is synthesized from 10μg of total RNA with the GeneChipT7-Oligo (dT) Promoter Primer Kit (Affymetrix, Inc.) and the SuperScript Choice System (Invitrogen). Biotin-labeled cRNA is then synthesized by in

vitro transcription using the BioArray High Yield RNA Transcript Labeling Kit (Affymetrix, Inc). After fragmentation, 15μg of labeled cRNA is hybridized to the oligonucleotide microarray. The chip is washed and stained using the GeneChip Fluidics Station 400 (Affymetrix) and then scanned with the GeneChip Scanner 3000 (Affymetrix). Resulting array images were processed with the Affymetrix Microarray Suite 5.0, and expression values were subsequently normalized and calculated with the PM-MM model using the DNA-Chip Analyzer (www.dchip.org). To classify a gene as significantly up-regulated or down-regulated, two additional criteria are used: (1) the fold change should be greater than or equal to 3 to be classified as increased or decreased and (2) genes that are classified as up-regulated should be flagged as present in the infected samples or herb and herb-derived treated samples, while genes that are classified as down-regulated should be flagged as present in the cells only control. All gene chip procedures are performed in replicates. Genes with significant transcriptional changes known to be associated with biological significance are selected for further analysis by real-time RT-PCR and immunoblotting analysis.

Real-time RT-PCR

Total RNA isolated from the above microarray experiment is reverse transcribed according to the manufacturer's protocols. Briefly, 1μg total RNA is mixed with 5mM $MgCl_2$, 1x PCR buffer, 4 mM each dNTP, RNase inhibitor, oligo dT and reverse transcriptase. The reaction is incubated at 42℃ for 60 min, 95℃ for 5 min and held at 4℃.

For each sample, primers for β-actin are included to determine the quality of the RNA. PCR primer pairs and the no. of universal probe used in the quantification of the genes are according to the Universal ProbeLibrary Assay Design Center from Roche applied science. PCR is perfromed using the FastStart TaqMan® Probe Master (Roche applied science), and the LightCycler 480 (Roche applied science). Monitoring the fluorescence of the reaction in real time allows the amplification to be halted when the sample is undergoing exponential growth making quantification of small differences possible. The reaction is stopped during the log phase to allow

for quantification of small differences.

Quantification of material labeled with SYBR green is analyzed by crossing point analysis, which represents the cycle number at which the sample begins exponential growth over the background noise. Data are presented in fluorescence versus cycle format in which all sample baselines are brought to a comparable level. Experiments are performed in duplicate and the result for an individual sample is expressed as the mean expression level of a specific gene relative to the reference cDNA. The relative expression between each infected sample and the cells only control is then calculated and expressed as fold change. Furthermore, the relative expression between each herb and herb-derived treated sample and the cells only control is also calculated and expressed as fold change.

Immunoblotting analysis

Protein samples are resolved by appropriate percentage of polyacrylamide gel electrophoresis. Subsequently, proteins in the gel are transferred onto the polyvinylidene difluoride (PVDF) membrane with a semi-dry transfer unit at 0.8 mA/cm^2 for 2h. The PVDF blots are blocked in TBST containing 2% non-fat dry milk, incubated with a primary antibody, followed by a secondary antibody conjugated with horseradish peroxidase. Proteins of interest are visualized with an ECL system followed by autoradiography.

Statistical analysis

The fold changes of the target gene expressions are compared by Student's *t* test. A *P* value of < 0.05 is considered significant. A statistical package (SPSS 10.0) is used for all analyses.

Protein preparation

Cells are harvested, washed twice with ice-cold PBS, resuspended and sonicated in extraction buffer containing 25mM Tris-HCl (pH 7.5), 2mM β-mercaptoethanol and the Complete, Mini, EDTA-free protease inhibitor mixture (Roche). After centrifugation at 10000*g* for 20 min,

ammonium sulfate is added to the supernatant until the final concentration reached 50% saturation w/v. The solution is stirred at 4℃ for 30 min and centrifuged at 10000*g* for 30min at 4℃. The supernatant fraction is then transferred into a fresh tube, and the precipitated protein pellet solubilized in extraction buffer. To remove salts and other contaminants, the extracts are treated with a pre-cooled (-20℃) solution of 10% TCA in acetone with 0.07% β-mercaptoethanol. Proteins are allowed to precipitate overnight at -20℃. After centrifugation, the pellet is washed with ice-cold acetone, containing 0.07% β-mercaptoethanol. The supernatant is discarded and the pellet dried in a vacuum centrifuge.

2-dimensional gel electrophoresis (2-DE)

The dried pellet is then extracted with lysis buffer containing 8 M urea, 4% CHAPS, 2% pH 3–10 non-linear (NL) IPG buffer (GE Healthcare), and the Complete, Mini, EDTA-free protease inhibitor mixture (Roche). After a 3-h incubation at 47C, the cell lysates are centrifuged for 15 min at 16000*g*. The protein concentration of the resulting supernatants is measured using the BioRad Protein Assay (BioRad, Hercules, CA, USA). Protein sample (100 mg) is diluted with 350 mL of rehydration buffer (8 M urea, 2% CHAPS, 0.5% IPG buffer pH 3–10 NL, 18 mM DTT, 0.002% bromophenol blue), and then applied to the nonlinear Immobiline DryStrips (17 cm, pH 3–10; GE Healthcare). After the run of 1-D IEF on a Multiphor II system (GE Healthcare), the gel strips are incubated for 30 min in the equilibration solution I (6 M urea, 2% SDS, 30% glycerol, 1% DTT, 0.002% bromophenol blue, 50 mM Tris-HCl, pH 8.8), and for another 30 min in the equilibration solution II (6 M urea, 2% SDS, 30% glycerol, 2.5% iodoacetamide, 0.002% bromophenol blue, 50 mM Tris-HCl, pH 8.8). Subsequently, the IPG gels are transferred to the top of 12% polyacrylamide gels (20 x 20 cm x 1.0 mm) for the secondary dimensional run at 15 mA, 300 V for 14 h.

Protein spot analysis

Separated protein spots are fixed in the fixing solution (40% ethanol and 10% glacial acetic acid) for 30 min, stained on the gel with silver nitrate solution for 20 min, and then scanned by GS-800 imaging densitometer with PDQuest software version 7.1.1 (BioRad). Data from three independently stained gels of each sample are exported to Microsoft Excel for creation of the correction graphs, spot intensity graphs and statistical analysis.

In-gel digestion

Each spot of interest in the silver-stained gel is sliced and put into the microtube, and then washed twice with 50% ACN in 100 mM ammonium bicarbonate buffer (pH 8.0) for 10 min at room temperature. Subsequently, the excised-gel pieces are soaked in 100% ACN for 5 min, dried in a lyophilizer for 30 min and rehydrated in 50 mM ammonium bicarbonate buffer (pH 8.0) containing 10 mg/mL trypsin at 307C for 16 h. After digestion, the peptides are extracted from the supernatant of the gel elution solution (50% ACN in 5.0% TFA), and dried in a vacuum centrifuge.

Nanoelectrospray MS and bioinformatics

The proteins are identified using an Ultimate capillary LC system (LC Packings, Amsterdam, The Netherlands) coupled to a QSTARXL quadrupole-time of flight (Q-TOF) mass spectrometer (Applied Biosystem/MDS Sciex, Foster City, CA, USA). The peptides are separated using an RP C18 capillary column (15 cm x 75 µm id) with a flow rate of 200 nL/min, and eluted with a linear ACN gradient from 10–50% ACN in 0.1% formic acid for 60 min. The eluted peptides from the capillary column are sprayed into the MS by a PicoTip electrospray tip (FS360-20-10-D-20; New Objective, Cambridge, MA, USA). Data acquisition from Q-TOF is performed using the automatic Information Dependent Acquisition (IDA; Applied Biosystem/MDS Sciex). Proteins are identified by the nanoLC-MS/MS spectra by searching against NCBI databases for exact matches using the ProID program (Applied Biosystem/MDS Sciex) and the MASCOT search program

(http://www.matrixscience.com). The protein function and subcellular location are annotated using the Swiss-Prot (http://us.expasy.org/sprot/). The proteins are also categorized according to their biological process and pathway using the PANTHER classification system (http://www.pantherdb.org).

結果與討論:

Identification of alternative cellular proteins induced by Kaempferol (Combined results from microarray and proteomic studies)

To identify cellular proteins induced by Kaempferol, which these cellular proteins may be involved in possible anti-EV71 mechanism, both microarray and proteomic studies were used to identify cellular proteins induced by Kaempferol. The results are shown in Figure 1, Table 1 and Table 2.

Our next step is to investigate the functions of these cellular proteins on anti-EV71 activity using siRNA and cDNA reconstruction assays.

參考文獻:

1. **Alexander, J. P., Jr., L. Baden, M. A. Pallansch, and L. J. Anderson.** 1994. Enterovirus 71 infections and neurologic disease--United States, 1977-1991. J Infect Dis **169:**905-8.
2. **Cassileth, B. R.** 1999. Alternative and complementary medicine. Separating the wheat from the chaff. Cancer **86:**1900-2.
3. **Chang, L. Y., T. Y. Lin, K. H. Hsu, Y. C. Huang, K. L. Lin, C. Hsueh, S. R. Shih, H. C. Ning, M. S. Hwang, H. S. Wang, and C. Y. Lee.** 1999. Clinical features and risk factors of pulmonary oedema after enterovirus-71-related hand, foot, and mouth disease. Lancet **354:**1682-6.
4. **Chonmaitree, T., M. A. Menegus, E. M. Schervish-Swierkosz, and E. Schwalenstocker.** 1981. Enterovirus 71 infection: report of an outbreak with two cases of paralysis and a review of the literature. Pediatrics **67:**489-93.
5. **Chumakov, M., M. Voroshilova, L. Shindarov, I. Lavrova, L. Gracheva, G. Koroleva, S. Vasilenko, I. Brodvarova, M. Nikolova, S. Gyurova, M. Gacheva, G. Mitov, N. Ninov, E. Tsylka, I. Robinson, M. Frolova, V. Bashkirtsev, L. Martiyanova, and V. Rodin.** 1979. Enterovirus 71 isolated from cases of epidemic poliomyelitis-like disease in Bulgaria. Arch Virol **60:**329-40.
6. **Conti, C., D. Genovese, R. Santoro, M. L. Stein, N. Orsi, and L. Fiore.** 1990. Activities

and mechanisms of action of halogen-substituted flavanoids against poliovirus type 2 infection in vitro. Antimicrob Agents Chemother **34:**460-6.

7. **Conti, C., P. Tomao, D. Genovese, N. Desideri, M. L. Stein, and N. Orsi.** 1992. Mechanism of action of the antirhinovirus flavanoid 4',6-dicyanoflavan. Antimicrob Agents Chemother **36:**95-9.
8. **Cummings, C. A., and D. A. Relman.** 2000. Using DNA microarrays to study host-microbe interactions. Emerg Infect Dis **6:**513-25.
9. **Dan, B., and G. Andrew.** 1986. Chinese Herbal Medicine, eighth ed. Eastland Press.
10. **Eisenberg, D. M., R. C. Kessler, C. Foster, F. E. Norlock, D. R. Calkins, and T. L. Delbanco.** 1993. Unconventional medicine in the United States. Prevalence, costs, and patterns of use. N Engl J Med **328:**246-52.
11. **Ernst, E., and B. R. Cassileth.** 1998. The prevalence of complementary/alternative medicine in cancer: a systematic review. Cancer **83:**777-82.
12. **Frydoonfar, H. R., D. R. McGrath, and A. D. Spigelman.** 2003. The variable effect on proliferation of a colon cancer cell line by the citrus fruit flavonoid Naringenin. Colorectal Dis **5:**149-52.
13. **Geiss, G. K., M. C. An, R. E. Bumgarner, E. Hammersmark, D. Cunningham, and M. G. Katze.** 2001. Global impact of influenza virus on cellular pathways is mediated by both replication-dependent and -independent events. J Virol **75:**4321-31.
14. **Geiss, G. K., V. S. Carter, Y. He, B. K. Kwieciszewski, T. Holzman, M. J. Korth, C. A. Lazaro, N. Fausto, R. E. Bumgarner, and M. G. Katze.** 2003. Gene expression profiling of the cellular transcriptional network regulated by alpha/beta interferon and its partial attenuation by the hepatitis C virus nonstructural 5A protein. J Virol **77:**6367-75.
15. **Genovese, D., C. Conti, P. Tomao, N. Desideri, M. L. Stein, S. Catone, and L. Fiore.** 1995. Effect of chloro-, cyano-, and amidino-substituted flavanoids on enterovirus infection in vitro. Antiviral Res **27:**123-36.
16. **Gilbert, G. L., K. E. Dickson, M. J. Waters, M. L. Kennett, S. A. Land, and M. Sneddon.** 1988. Outbreak of enterovirus 71 infection in Victoria, Australia, with a high incidence of neurologic involvement. Pediatr Infect Dis J **7:**484-8.
17. **Hayward, J. C., S. M. Gillespie, K. M. Kaplan, R. Packer, M. Pallansch, S. Plotkin, and L. B. Schonberger.** 1989. Outbreak of poliomyelitis-like paralysis associated with enterovirus 71. Pediatr Infect Dis J **8:**611-6.
18. **Heasman, J.** 2002. Morpholino oligos: making sense of antisense? Dev Biol **243:**209-14.
19. **Ho, M., E. R. Chen, K. H. Hsu, S. J. Twu, K. T. Chen, S. F. Tsai, J. R. Wang, and S. R. Shih.** 1999. An epidemic of enterovirus 71 infection in Taiwan. Taiwan Enterovirus Epidemic Working Group. N Engl J Med **341:**929-35.
20. **Huang, C. C., C. C. Liu, Y. C. Chang, C. Y. Chen, S. T. Wang, and T. F. Yeh.** 1999. Neurologic complications in children with enterovirus 71 infection. N Engl J Med

341:936-42.

21. **Ishimaru, Y., S. Nakano, K. Yamaoka, and S. Takami.** 1980. Outbreaks of hand, foot, and mouth disease by enterovirus 71. High incidence of complication disorders of central nervous system. Arch Dis Child **55:**583-8.
22. **Jacque, J. M., K. Triques, and M. Stevenson.** 2002. Modulation of HIV-1 replication by RNA interference. Nature **418:**435-8.
23. **Kennett, M. L., C. J. Birch, F. A. Lewis, A. P. Yung, S. A. Locarnini, and I. D. Gust.** 1974. Enterovirus type 71 infection in Melbourne. Bull World Health Organ **51:**609-15.
24. **Konoshima, T., M. Kokumai, M. Kozuka, M. Iinuma, M. Mizuno, T. Tanaka, H. Tokuda, H. Nishino, and A. Iwashima.** 1992. Studies on inhibitors of skin tumor promotion. XI. Inhibitory effects of flavonoids from Scutellaria baicalensis on Epstein-Barr virus activation and their anti-tumor-promoting activities. Chem Pharm Bull (Tokyo) **40:**531-3.
25. **Korth, M. J., and M. G. Katze.** 2002. Unlocking the mysteries of virus-host interactions: does functional genomics hold the key? Ann N Y Acad Sci **975:**160-8.
26. **Lin, C. W., F. J. Tsai, C. H. Tsai, C. C. Lai, L. Wan, T. Y. Ho, C. C. Hsieh, and P. D. Chao.** 2005. Anti-SARS coronavirus 3C-like protease effects of Isatis indigotica root and plant-derived phenolic compounds. Antiviral Res **68:**36-42.
27. **Lin, T. Y., S. J. Twu, M. S. Ho, L. Y. Chang, and C. Y. Lee.** 2003. Enterovirus 71 outbreaks, Taiwan: occurrence and recognition. Emerg Infect Dis **9:**291-3.
28. **Lum, L. C., K. T. Wong, S. K. Lam, K. B. Chua, A. Y. Goh, W. L. Lim, B. B. Ong, G. Paul, S. AbuBakar, and M. Lambert.** 1998. Fatal enterovirus 71 encephalomyelitis. J Pediatr **133:**795-8.
29. **Manthey, J. A., and N. Guthrie.** 2002. Antiproliferative activities of citrus flavonoids against six human cancer cell lines. J Agric Food Chem **50:**5837-43.
30. **McManus, M. T., and P. A. Sharp.** 2002. Gene silencing in mammals by small interfering RNAs. Nat Rev Genet **3:**737-47.
31. **Nagy, G., S. Takatsy, E. Kukan, I. Mihaly, and I. Domok.** 1982. Virological diagnosis of enterovirus type 71 infections: experiences gained during an epidemic of acute CNS diseases in Hungary in 1978. Arch Virol **71:**217-27.
32. **Novina, C. D., M. F. Murray, D. M. Dykxhoorn, P. J. Beresford, J. Riess, S. K. Lee, R. G. Collman, J. Lieberman, P. Shankar, and P. A. Sharp.** 2002. siRNA-directed inhibition of HIV-1 infection. Nat Med **8:**681-6.
33. **Pattanakitsakul, S. N., K. Rungrojcharoenkit, R. Kanlaya, S. Sinchaikul, S. Noisakran, S. T. Chen, P. Malasit, and V. Thongboonkerd.** 2007. Proteomic Analysis of Host Responses in HepG2 Cells during Dengue Virus Infection. J Proteome Res **6:**4592-600.
34. **Salvati, A. L., A. De Dominicis, S. Tait, A. Canitano, A. Lahm, and L. Fiore.** 2004. Mechanism of action at the molecular level of the antiviral drug 3(2H)-isoflavene against type 2 poliovirus. Antimicrob Agents Chemother **48:**2233-43.

35. **Samuda, G. M., W. K. Chang, C. Y. Yeung, and P. S. Tang.** 1987. Monoplegia caused by Enterovirus 71: an outbreak in Hong Kong. Pediatr Infect Dis J **6:**206-8.
36. **Scheel, J., M. C. Von Brevern, A. Horlein, A. Fischer, A. Schneider, and A. Bach.** 2002. Yellow pages to the transcriptome. Pharmacogenomics **3:**791-807.
37. **Schlee, M., T. Krug, O. Gires, R. Zeidler, W. Hammerschmidt, R. Mailhammer, G. Laux, G. Sauer, J. Lovric, and G. W. Bornkamm.** 2004. Identification of Epstein-Barr virus (EBV) nuclear antigen 2 (EBNA2) target proteins by proteome analysis: activation of EBNA2 in conditionally immortalized B cells reflects early events after infection of primary B cells by EBV. J Virol **78:**3941-52.
38. **Smith, M. W., Z. N. Yue, M. J. Korth, H. A. Do, L. Boix, N. Fausto, J. Bruix, R. L. Carithers, Jr., and M. G. Katze.** 2003. Hepatitis C virus and liver disease: global transcriptional profiling and identification of potential markers. Hepatology **38:**1458-67.
39. **Sparber, A., and J. C. Wootton.** 2001. Surveys of complementary and alternative medicine: Part II. Use of alternative and complementary cancer therapies. J Altern Complement Med **7:**281-7.
40. **Surabhi, R. M., and R. B. Gaynor.** 2002. RNA interference directed against viral and cellular targets inhibits human immunodeficiency Virus Type 1 replication. J Virol **76:**12963-73.
41. **Thyagarajan, S. P., S. Subramanian, T. Thirunalasundari, P. S. Venkateswaran, and B. S. Blumberg.** 1988. Effect of Phyllanthus amarus on chronic carriers of hepatitis B virus. Lancet **2:**764-6.
42. **Venkateswaran, P. S., I. Millman, and B. S. Blumberg.** 1987. Effects of an extract from Phyllanthus niruri on hepatitis B and woodchuck hepatitis viruses: in vitro and in vivo studies. Proc Natl Acad Sci U S A **84:**274-8.

計劃成果自評部份:

本計劃研究內容與原計劃相符。我們先前已利用 microarray and proteomic 方法找出與 EV71 感染相關蛋白。目前已利用相同方法，找出與 Kaempferol 藥物相關的細胞蛋白。利用 siRNA 與 cDNA reconstruction assays，我們要証明這些 candidate 細胞蛋白在抗 EV71 之中藥相關研究上有幫助。我們有達成預期目標。其研究成果具學術價值，適合在學術期刊發表。

Figure 1

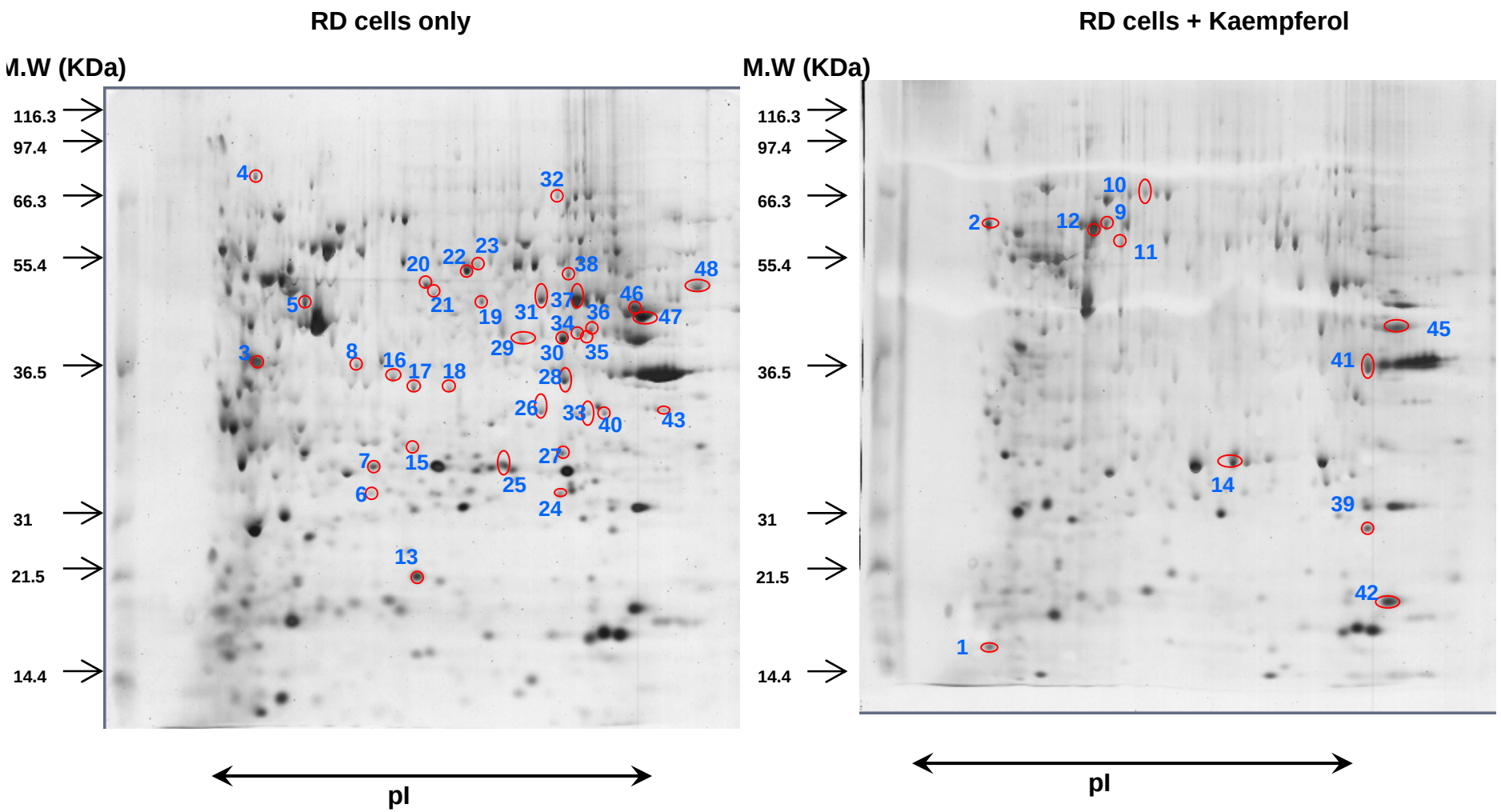
RD cells only
M.W (KDa)
116.3
97.4
66.3
55.4
36.5
31
21.5
14.4
pI
RD cells + Kaempferol
M.W (KDa)
116.3
97.4
66.3
55.4
36.5
31
21.5
14.4
pI

Table 1. Identified altered proteins in the RD cells induced by Kaempferol (Proteomic studies)

Spot no.	Protein name	Protein description	Accession no.	Panther Gene ID	Score	Sequence coverage (%)	MW (KDa)/p*I*
K1	MYL6_HUMAN	Myosin light polypeptide 6	P60660	4637	246	62	16.9/4.56
K2	CALR_HUMAN	Calreticulin precursor - Homo sapiens (Human)	P27797	811	1034	71	48.1/4.29
K3	HNRPC_HUMAN	Heterogeneous nuclear ribonucleoproteins C1/C2 - Homo sapiens (Human)	P07910	3183	186	23	33.6/4.95
K4	ENPL_HUMAN	Endoplasmin precursor - Homo sapiens (Human)	P14625	7184	837	36	92.4/4.76
K5	HNRPF_HUMAN	Heterogeneous nuclear ribonucleoprotein F - Homo sapiens (Human)	P52597	3185	128	15	45.6/5.38
K6	GSTP1_HUMAN	Glutathione S-transferase P - Homo sapiens (Human)	P09211	2950	618	57	23.3/5.43
K7	HSPB1_HUMAN	Heat shock protein beta-1 - Homo sapiens (Human)	P04792	3315	299	51	22.7/5.98
K8	IF32_HUMAN	Eukaryotic translation initiation factor 3 subunit 2 - Homo sapiens (Human)	CAD25741		510	69	36.4/5.38
K9	CH60_HUMAN	60 kDa heat shock protein, mitochondrial precursor - Homo sapiens (Human)	P10809	3329	1140	65	61.0/5.70
K10	ALBU_HUMAN	Serum albumin precursor - Homo sapiens (Human)	P02768	213	132	8	69.3/5.92
K11	TCPQ_HUMAN	T-complex protein 1 subunit theta - Homo sapiens (Human)	P50990	10694	1079	64	59.5/5.42
K12	HNRPK_HUMAN	Heterogeneous nuclear ribonucleoprotein K - Homo sapiens (Human)	P61978	3190	483	37	50.9/5.39
K13	NDKA_HUMAN	Nucleoside diphosphate kinase A - Homo sapiens (Human)	P15531	4830	558	85	17.1/5.83
K14	CN166_HUMAN	Protein C14orf166 - Homo sapiens (Human)	Q9Y224	51637	514	73	28.0/6.19
K15	PSB7_HUMAN	Proteasome subunit beta type-7 precursor - Homo sapiens	Q99436	5695	247	36	29.9/7.57
K16	LDHB_HUMAN	L-lactate dehydrogenase B chain - Homo sapiens (Human)	P07195	3945	390	40	36.6/5.71
K17	NADC_HUMAN	Nicotinate-nucleotide pyrophosphorylase [carboxylating] - Homo sapiens (Human)	Q15274	23475	236	31	30.7/5.81
K18	PSDE_HUMAN	26S proteasome non-ATPase regulatory subunit 14 - Homo sapiens (Human)	O00487	10213	116	18	34.5/6.06
K19	PA2G4_HUMAN	Proliferation-associated protein 2G4 - Homo sapiens (Human)	Q9UQ80	5036	465	54	43.7/6.13
K20	PRS7_HUMAN	26S protease regulatory subunit 7 - Homo sapiens (Human)	P35998	5701	474	59	48.6/5.71
K21	HNRH1_HUMAN	Heterogeneous nuclear ribonucleoprotein H - Homo sapiens (Human)	P31943	3187	423	35	49.2/5.89
K22	TCPB_HUMAN	T-complex protein 1 subunit beta - Homo sapiens (Human)	P78371	10576	1973	76	57.5/6.01
K23	AL1B1_HUMAN	Aldehyde dehydrogenase X, mitochondrial precursor - Homo s	P30837	219	349	31	57.2/6.36
K24	LYPA2_HUMAN	Acyl-protein thioesterase 2 - Homo sapiens (Human)	O95372	11313	91	22	24.7/6.75
K25	PSA6_HUMAN	Proteasome subunit alpha type-6 - Homo sapiens (Human)	P60900	5687	321	41	27.4/6.34
K26	ESTD_HUMAN	S-formylglutathione hydrolase - Homo sapiens (Human)	P10768	2098	280	39	31.4/6.54
K27	PGAM1_HUMAN	Phosphoglycerate mutase 1 - Homo sapiens (Human)	P18669	5223	545	77	28.7/6.67
K28	CNN2_HUMAN	Calponin-2 - Homo sapiens (Human)	Q99439	1265	217	20	33.7/6.95
K29	RBM4_HUMAN	RNA-binding protein 4 - Homo sapiens (Human)	Q9BWF3	5936	254	34	40.3/6.61
K30	ALDOC_HUMAN	Fructose-bisphosphate aldolase C - Homo sapiens (Human)	P09972	230	91	8	39.4/6.41
K31	EFTU_HUMAN	Elongation factor Tu, mitochondrial precursor - Homo sapiens	P49411	7284	247	30	49.5/7.26
K32	FUBP2_HUMAN	Far upstream element-binding protein 2 - Homo sapiens (Huma	Q92945	8570	499	25	73.1/6.84
K33	GBLP_HUMAN	Guanine nucleotide-binding protein subunit beta-2-like 1 - Hon	P63244	10399	103	13	35.0/7.60
K34	PPID_HUMAN	40 kDa peptidyl-prolyl cis-trans isomerase - Homo sapiens (Hu	Q08752	5481	488	48	40.7/6.77
K35	TOM40_HUMAN	Probable mitochondrial import receptor subunit TOM40 homo	O96008	10452	62	6	37.8/6.79
K35	MAT2B_HUMAN	Methionine adenosyltransferase 2 subunit beta - Homo sapiens	Q9NZL9	27430	57	5	37.5/6.90
K36	HNRPD_HUMAN	Heterogeneous nuclear ribonucleoprotein D0 - Homo sapiens (H	Q14103	3184	229	22	38.4/7.62
K37	ENOA_HUMAN	Alpha-enolase - Homo sapiens (Human)	P06733	2023	3442	66	47.1/7.01
K38	FSCN1_HUMAN	Fascin - Homo sapiens (Human)	Q16658	6624	776	57	54.5/6.84
K39	PEBP1_HUMAN	Phosphatidylethanolamine-binding protein 1 - Homo sapiens (H	P30086	5037	597	79	
K40	GBLP_HUMAN	Guanine nucleotide-binding protein subunit beta-2-like 1 - Hon	P63244	10399	512	70	35.0/7.60
K41	MTDC_HUMAN	Bifunctional methylenetetrahydrofolate dehydrogenase/cycloh	P13995	10797	158	22	37.8/8.86
K42	RT28_HUMAN	Mitochondrial 28S ribosomal protein S28 - Homo sapiens (Hun	Q9Y2Q9	28957	201	36	20.8/9.21
K43	VDAC1_HUMAN	Voltage-dependent anion-selective channel protein 1 - Homo sa	P21796	7416	475	61	30.7/8.62
K45	ALDOA_HUMAN	Fructose-bisphosphate aldolase A - Homo sapiens (Human)	P04075	226	838	71	39.4/8.30
K46	THIM_HUMAN	3-ketoacyl-CoA thiolase, mitochondrial - Homo sapiens (Huma	P42765	10449	487	49	41.9/8.32
K47	PGK1_HUMAN	Phosphoglycerate kinase 1 - Homo sapiens (Human)	P00558	6654	1009	70	44.6/8.30
K48	EF1A1_HUMAN	Elongation factor 1-alpha 1 - Homo sapiens (Human)	P68104	1915	406	29	50.1/9.10

Table 2. Identified altered proteins in the RD cells induced by Kaempferol (Microarray studies)

probe set	gene	Accession	LocusLin	Descripti	RD-1	RD-2	baseline mean	line mean	RD and K-1	RD and K-2	RD and K-3	ent mean	nean's SE	fold change	r bound o	r bound o	ence of n
226699_at	FCHSD1: FCH and double SH3 domains 1	AK000007	89848	gb:AK00	368.68	535.72	451.27	84.53	17.71	17.92	-49.15	-1.62	27.49	-451.27	-9.28	-1E+08	-452.89
207282_s_at	MYOG: myogenin (myogenic factor 4)	NM_002479	4656	gb:NM_0	335.78	480.48	408.71	73.02	-2.23	-16	-63.92	-27.07	28.85	-408.71	-8.05	-1E+08	-435.77
222278_at	Transcribed locus, strongly similar to XP_374169.2 PREDICTED: hypothetical protein XP_37416	AW969655		gb:AW96	258.82	391.72	325.07	68.28	33.19	22.18	-0.52	19.62	23.92	-16.57	-5.01	-1E+08	-305.45
207022_s_at	LDHC: lactate dehydrogenase C	NM_002301	3948	gb:NM_0	109.08	133.13	121.4	13.95	15.64	11.69	14.75	13.73	13.12	-8.84	-3.34	-1E+08	-107.67
206393_at	TNNI2: troponin I type 2 (skeletal, fast)	NM_003282	7136	gb:NM_0	188.47	181.59	184.18	13.46	49.97	4.7	30.72	27.14	16	-6.79	-3.39	-224.76	-157.04
230626_at	TSPAN12: tetraspanin 12	AI056699	23554	gb:AI056	472.08	421.16	448.1	28.85	51.6	83.61	84.03	74.19	13.32	-6.04	-4.55	-8.68	-373.9
201008_s_at	TXNIP: thioredoxin interacting protein	AA812232	10628	gb:AA81	419.02	352.16	386.3	38.78	53.52	121.48	26.2	67.51	32.85	-5.72	-3.08	-28.77	-318.79
225301_s_at	MYO5B: myosin VB	AI991160	4645	gb:AI991	705.5	972.03	832.63	140.56	191.04	129.9	177.79	163.18	27.16	-5.1	-3.41	-7.63	-669.45
210512_s_at	VEGF: vascular endothelial growth factor	AF022375	7422	gb:AF022	406.24	464.03	434.66	33.73	1760.73	1380.81	1735.44	1624.12	124.68	3.74	3.12	4.48	1189.46
202847_at	PCK2: phosphoenolpyruvate carboxykinase 2 (mitochondrial)	NM_004563	5106	gb:NM_0	460.15	465.9	462.52	33.06	2039.05	1411.81	1918.61	1788.04	193.19	3.87	3.09	4.75	1325.52
209967_s_at	CREM: cAMP responsive element modulator	D14826	1390	gb:D1482	619.41	568.19	589.34	34.72	2063.2	2311.1	2691.11	2360.95	192.95	4.01	3.38	4.71	1771.61
203140_at	BCL6: B-cell CLL/lymphoma 6 (zinc finger protein 51) /// B-cell CLL/lymphoma 6 (zinc finger pr	NM_001706	604	gb:NM_0	98.42	104.73	102.38	8.68	436.56	325.04	480.75	413.81	47.36	4.04	3.16	5.08	311.44
225442_at	Clone DPDP-3 dental pulp-derived protein 3, mRNA sequence	AI799915		gb:AI799	576.59	652.43	613.31	43.93	2940.1	2291.89	2433.95	2556.02	198.25	4.17	3.5	4.96	1942.72
223195_s_at	SESN2: sestrin 2	BF131886	83667	gb:BF131	123.96	119.53	122.14	15.14	572.08	384.47	580.62	511.65	65.33	4.19	3.11	5.64	389.51
215318_at	CG012: hypothetical gene CG012	AL049782	116829	gb:AL049	39.92	37.93	38.76	6.54	205.6	128.13	181.76	171.21	23.61	4.42	3.1	6.48	132.46
205047_s_at	ASNS: asparagine synthetase	NM_001673	440	gb:NM_0	1261.01	1426.64	1349.2	116.9	6587.14	6292.36	5967.2	6269.86	238.05	4.65	4.01	5.48	4920.67
223218_s_at	NFKBIZ: nuclear factor of kappa light polypeptide gene enhancer in B-cells inhibitor, zeta	AB037925	64332	gb:AB037	332.59	283.85	307.13	29.22	1645.56	1558.37	1370.48	1525.46	85.14	4.97	4.17	6.01	1218.33
207850_at	CXCL3: chemokine (C-X-C motif) ligand 3	NM_002090	2921	gb:NM_0	31.28	48.72	39.49	10.73	184.05	208.68	244.92	214.79	22.54	5.44	3.58	10.01	175.3
224917_at	MIRN21: microRNA 21	BF674052	406991	gb:BF674	178.7	162.71	169.33	20.29	1078.46	1185.2	579.46	946.7	189.63	5.59	3.62	8.02	777.37
202237_at	NNMT: nicotinamide N-methyltransferase	NM_006169	4837	gb:NM_0	138.5	82.43	110.23	28.92	599.51	483.22	827.16	636.28	102.2	5.77	3.6	10.59	526.06
227062_at	TncRNA: trophoblast-derived noncoding RNA	AU155361	283131	gb:AU155	258.35	197.5	227.38	48.48	1287.25	1151.25	1514.72	1317.01	117.53	5.79	4.12	9.09	1089.63
228661_s_at	CDNA FLJ11489 fis, clone HEMBA1001915	AI768374		gb:AI768	99.91	78.35	88.73	16.21	606.32	336.92	619.26	519.41	93.25	5.85	3.78	9.08	430.68
223217_s_at	NFKBIZ: nuclear factor of kappa light polypeptide gene enhancer in B-cells inhibitor, zeta	BE646573	64332	gb:BE646	94.13	73.56	83.71	36.73	693.28	415.29	487.48	528.11	85.91	6.31	3.36	22.98	444.4
232240_at	CCDC35: coiled-coil domain containing 35	T85902	387750	gb:T8590	179.67	90.71	136.13	59.7	925.76	656.89	1125.47	900.49	141.39	6.61	3.54	24.04	764.35
203708_at	PDE4B: phosphodiesterase 4B, cAMP-specific (phosphodiesterase E4 dunce homolog, Drosophila	NM_002600	5142	gb:NM_0	74.22	72.86	73.58	8.35	448.97	426.88	596.12	494.04	59.19	6.71	5.09	8.83	420.46
202859_x_at	IL8: interleukin 8	NM_000584	3576	gb:NM_0	94.74	94.15	94.46	10.67	1050.9	340.31	644.46	678.01	205.72	7.18	3.54	11.33	583.55
205266_at	LIF: leukemia inhibitory factor (cholinergic differentiation factor)	NM_002309	3976	gb:NM_0	32.06	17.33	24.2	11.32	175.65	192.29	193.64	187.96	13.22	7.77	4.32	33.73	163.76
231202_at	ALDH1L2: aldehyde dehydrogenase 1 family, member L2	AI654224	160428	gb:AI654	79.05	104.34	90.31	15.09	869.5	478.19	836.03	727.38	125.34	8.05	5.34	12.08	637.06
230135_at	CDNA FLJ42405 fis, clone ASTRO3000474	AI822137		gb:AI822	13.47	22.05	17.44	10.46	227.98	77.6	152.75	152.52	43.42	8.74	3.43	626.79	135.07
214079_at	DHRS2: dehydrogenase/reductase (SDR family) member 2	AK000345	10202	gb:AK00	19.44	6.45	14.22	10.7	189.65	91.84	109.94	130.26	30.57	9.16	3.54	1E+08	116.04
206157_at	PTX3: pentraxin-related gene, rapidly induced by IL-1 beta	NM_002852	5806	gb:NM_0	34.1	24.83	29.69	6.55	346.92	158.28	373.02	292.03	68.19	9.84	5.55	17.11	262.34
230147_at	F2RL2: coagulation factor II (thrombin) receptor-like 2	AI378647	2151	gb:AI378	19.41	32.55	26.38	8.2	470.11	191.53	263.14	307.02	83.44	11.64	5.68	25.83	280.64
210587_at	INHBE: inhibin, beta E	BC005161	83729	gb:BC005	49.4	41.95	45.24	7.37	740.36	400.72	515.74	551.82	99.46	12.2	7.99	18.29	506.58
204971_at	CSTA: cystatin A (stefin A)	NM_005213	1475	gb:NM_0	27.27	32.87	29.92	5.8	418.77	716.98	1251.31	795.88	245.49	26.6	12.53	46.68	765.96
221577_x_at	GDF15: growth differentiation factor 15	AF003934	9518	gb:AF003	166.78	145.15	155.78	21.87	4639.8	4705.89	3151.69	4163.49	520.54	26.73	19.61	36.86	4007.71
217678_at	SLC7A11: solute carrier family 7, (cationic amino acid transporter, y+ system) member 11	AA488687	23657	gb:AA488	24.61	41.96	32.7	11.64	2988.71	1596.13	1508.68	2026.92	482.82	61.98	31.49	157.17	1994.22
209921_at	SLC7A11: solute carrier family 7, (cationic amino acid transporter, y+ system) member 11	AB040875	23657	gb:AB040	15.39	32.31	25.68	25.68	2870.8	1748.32	1904.66	2175.45	350.24	84.71	30.2	1E+08	2149.77
221173_at	USH1C: Usher syndrome 1C (autosomal recessive, severe)	NM_025034	10083	gb:NM_0	0.78	2.62	1.79	13.38	361.89	65.87	205.81	211.24	85.06	118.12	6.47	1E+08	209.45
219270_at	CHAC1: ChaC, cation transport regulator-like 1 (E. coli)	NM_024111	79094	gb:NM_0	-2.34	0.59	-0.64	14.27	114.57	328.72	257.12	234.72	67.24	234.72	8.41	1E+08	235.36